IMPROVEMENT OF A RADIATION PROCESS FOR THE NON-HYDROSTATIC MODEL

P2.10

Ryoji Nagasawa*
Numerical Prediction Division, Japan Meteorological Agency, Tokyo, Japan

1. INTRODUCTION

The Japan Meteorological Agency has developed a non-hydrostatic model (NHM). The NHM began to be used in operational in October 2004 (Saito et al, 2006). Horizontal resolution of the operational NHM was increased from 10 km to 5km in March 2006.

In meso-scale model, the radiation process is important in terms of forecast of surface air temperature, low-level clouds and fog. Current radiation scheme of the NHM is Kitagawa (2000) with diagnosed cloud fraction of Ohno and Isa (1984). But the diagnosed cloud fraction tends to spread wider than actual cloud distribution, and then the excessive cloud distribution suppresses downward shortwave radiation fluxes at surface. This is one of the reasons that simulated surface air temperature by the NHM has negative bias in day time to surface observation. In order to ameliorate the problem, a new cloud fraction diagnostic method; Hack (1998) with adjustment for high-resolution simulation are tested.

2. CLOUD FRACTION DIAGNOSTIC METHOD

In this study, a new cloud fraction diagnostic method (Hack 1998) are tested which had been used in the NCAR CCM2 (Community Climate Model Ver. 2) with some adjustments for high-resolution model. This method is based on the cloud fraction diagnostic method of Slingo (1987). The cloud fraction depends on the relative humidity, vertical velocity, atmospheric stability and convective precipitation rate. In the method, convective cloud, layered cloud and marine low-level cloud are diagnosed.

In Hack (1998), convective cloud fraction A_{conv} is diagnosed on the basis of the convective precipitation rate using

$$A_{conv} = 0.20 + 0.125\ln(1.0 + P) \quad (1)$$

where P is the convective precipitation rate in mm / day by the convective parameterization scheme.

The relative humidity within the grid box is then adjusted to account for the assumption that the fractional area of convective cloud, A_{conv}, is saturated. This adjusted relative humidity, RH', is given by

$$RH' = \frac{RH - A_{conv}}{1 - A_{conv}} \quad (2)$$

where RH is the original relative humidity.

In this high-resolution simulation, frontal and tropical low-level cloud in Hack (1998) is treated as just low-level layered cloud to avoid much unnatural low-level cloud. Therefore low-, middle-, high-level layered cloud fraction is determined from the relation

$$A_c = \left[\max\left(0, \frac{RH' - RH_{\lim}}{1 - RH_{\lim}}\right)\right]^2 \quad (3)$$

where

$$RH_{\lim} = 0.999 - fact \times \left[1 - \frac{N^2}{2.5\times10^{-4}}\right], \quad (4)$$

N^2 is the square of the Brunt-Vaisala frequency. Further, the experimental parameter for high-resolution simulation $fact$ is introduced to reproduce reasonable cloud fraction.

Marine low-level cloud with boundary inversion is determined as follows:

$$A_c = 0 \qquad (RH' < 0.6,\ p_{inv} \le p \le p_s)$$

$$= \left(-6.67\frac{\partial\theta}{\partial p} - 0.667\right) \times \left(1 - \frac{0.9 - RH'}{0.3}\right) \times \left(\frac{p_s - p}{p_s - p_{iinv}}\right)$$

$$(0.6 \le RH' \le 0.9 \ and \ \frac{\partial\theta}{\partial p} < -0.125,\ p_{inv} \le p \le p_s)$$

$$= \left(-6.67\frac{\partial\theta}{\partial p} - 0.667\right) \times \left(\frac{p_s - p}{p_s - p_{inv}}\right)$$

$$(RH' > 0.9 \ \ and \ \ \frac{\partial\theta}{\partial p} < -0.125,\ p_{inv} \le p \le p_s) \quad (6)$$

where $\frac{\partial\theta}{\partial p}$ is the maximum inversion strength, p is pressure in any layer, p_s is surface pressure, p_{inv} is pressure at the level with maximum inversion strength.

* *Corresponding author: Ryoji Nagasawa, Japan Meteorological Agency, 1-3-4 Otemachi, Chiyoda-ku, Tokyo 100-8122, Japan; e-mail: r-nagasawa@met.kishou.go.jp*

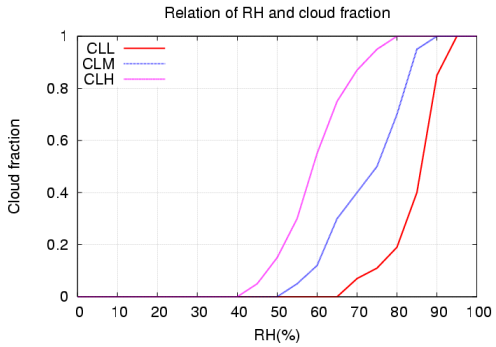

Fig. 1. Statistical relation between cloud fraction and relative humidity of Ohno and Isa (1984). CLL: low-level cloud, CLM: middle-level cloud, CLH: high-level cloud, RH: relative-humidity

Table1. Outline of the experiment

Experimental period	From 12 to 17 July 2004
Initial times	00, 12 UTC
Integration time	24 hours
Horizontal resolution	5km
Initial condition	Operational meso analysis
Lateral boundary condition	Forecasts of JMA Regional Spectral Model
Radiation scheme	Kitagawa (2000)

The total cloud fraction in any layer is defied as

$$A_c = (1.0 - A_{conv})A_c + A_{conv} \quad (7)$$

On the other hand, current cloud fraction diagnostic method: Ohno and Isa (1984) diagnoses cloud fraction following the statistical relation between relative humidity and low-, middle-, high-level cloud fraction (Fig. 1).

In both cloud fraction diagnostic methods, cloud water content is diagnosed from precipitable water amount following the cloud water diagnostic method in Hack (1998) as follows;

$$\rho_l = \rho_l^0 e^{(-z/h_l)} \quad (8)$$

$$h_l = 700(1.0 + TPW) \quad (9)$$

where ρ_l is cloud water content、ρ_l^0 is equal to 0.21 (gm^{-3}) Z is height (m), and TPW is precipitable water (kgm^{-2}).

3. RADIATION SCHEME (KITAGAWA, 2000)

The shortwave radiation scheme of the NHM is based on the 18-band model of Briegleb (1992) using the *k*-distribution method. Cloud optical parameters such as optical depth, single scattering albedo and asymmetry factor are estimated from cloud water content and an assumed effective cloud-particle radius (Slingo 1989, Ebert and Curry, 1992).

For the longwave radiation, the total spectral region is divided into four broad bands, and water vapor and carbon dioxide absorption parameters in each band are determined by the random model (Goody 1952). Basically, clouds are assumed to be a black body. But in order to proper treatment of the effects of optically thin high level-clouds, cloud fraction is corrected by emissivity diagnosed by cloud water and ice content, effective radius, following Kiehl and Zender (1995).

Typical vertical profiles of optical properties are used for marine-type and land-type aerosols.

4. EXPERIMENTAL DESIGN AND RESULTS

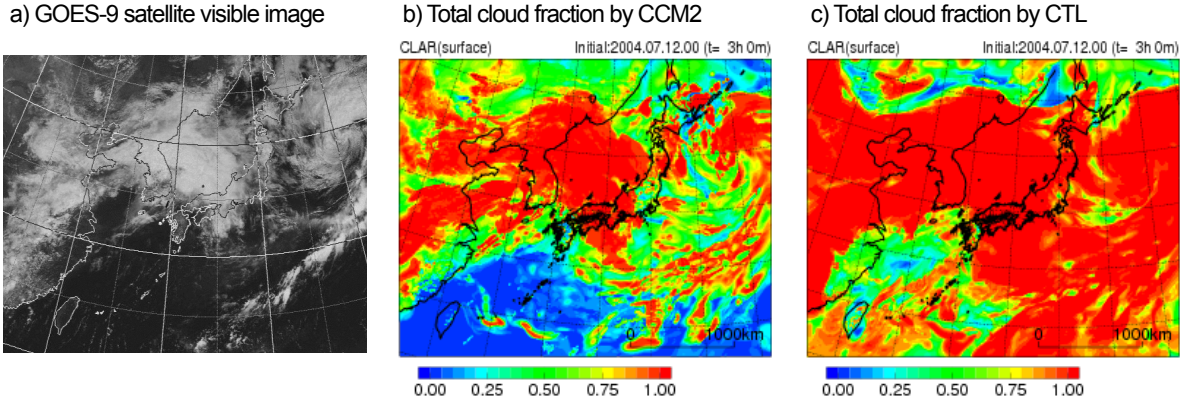

Fig. 2. a) GOES-9 satellite visible image at 03 UTC on 12 July 2004 and total cloud fraction simulated by b) CCM2, c) CTL at 3 hour after the initial time (00 UTC on 12 July 2004).

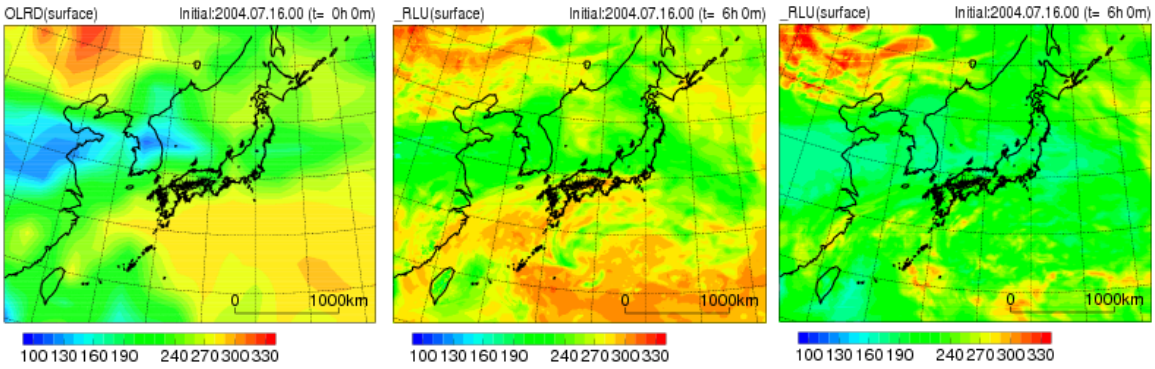

Fig.3. a) Outgoing longwave radiation flux (Wm^{-2}) at top of the atmosphere at around 06 UTC on 16 July 2004 observed by NOAA-16 and upward longwave radiation flux at top of the atmosphere simulated by b) CCM2, c) CTL at 6 hour after the initial time (00 UTC on 16 July 2004).

To investigate the impact of the new cloud fraction diagnostic method, impact experiments are executed. Control run which uses cloud fraction diagnosed by Ohno and Isa (1984) is CTL and a test run which uses cloud fraction diagnosed by Hack (1998) is CCM2. In both CCM2 and CTL, the radiation scheme of Kitagawa (2000) is used. Experimental period is from 12 to 17 July 2004. Horizontal resolution of the NHM is 5 km. The outline of the experiment is summarized in Table. 1 and computational domain is same as the area of Fig. 2 b), c).

Figure 2 a) shows GOES-9 satellite visible image at 03 UTC on 12 July 2004. In northern and eastern Japan, low-level clouds are remarkable. Further, around the Japan sea, middle- and high-level clouds by warm front are remarkable. Figure 2 b) and c) show total cloud fraction simulated by CCM2 and CTL at the same valid time, respectively. CTL simulates general features of actual cloud distribution. But cloud distribution is too wide and clear area in Fig. 2 a) is simulated as cloudy area. On the other hand, in CCM2, clear area in the southern part of the computational domain in Fig. 2 a) are simulated and on the whole, cloud distribution is narrower than CTL. If partial cloud fraction area is ignored, cloud distribution in CCM2 is close to the actual cloud distribution.

Next, the impact of improvement of cloud distribution to outgoing longwave radiation flux at top of the atmosphere (hereafter OLR) is shown. Figure 3 a) shows OLR at 06 UTC on 16 July 2004 observed by NOAA-16. Figure 3 b), c) shows OLR simulated by CCM2 and CTL at the same valid time. In CTL, value of OLR as a whole is smaller than that in observation. On the other hand, in CCM2, high OLR areas correspond to sub-high, off the east coast of Hokkaido, the Japan sea are well simulated. In observation, low OLR areas exist in Korean peninsula and Chinese continent. These areas can not be simulated even in CCM2. Cloud top height of the diagnosed cloud in CCM2, value of the diagnosed cloud water content, and method of radiation calculation still have errors.

Finally, the impact of improvement of cloud distribution to downward shortwave radiation flux at surface (hereafter DSWB) is shown. In CTL, DSWB has negative bias to surface observations whose maximum value is about 200 Wm^{-2}, because cloud distribution is too wide (Fig. 4 a)). Negative bias of the DSWB is thought to be one of the reasons of the negative bias of the surface air temperature. On the other hand, in CCM2, magnitude of the bias of the DSWB decreased to about 50 Wm^{-2}. The RMSE in CCM2 is smaller than that in CTL (Fig. 4 b)). In brief, forecast of DSWB is improved in CCM2. In standard deviation, magnitude of CTL and CCM2 is almost same (Fig. 4 c)). Therefore improvement of Mean Error in CCM2 contributes to the improvement of RMSE in CCM2.

5. SUMMARY

A new cloud fraction diagnostic method based on Hack (1998) was tested and was compared with the current cloud fraction diagnostic method (Ohno and Isa, 1984). Using the new method, cloud distribution, pattern of OLR and forecast of DSWB were improved compared to those of current method. More refinement of the cloud fraction diagnostic method and effective use of predicted cloud variables remain future works.

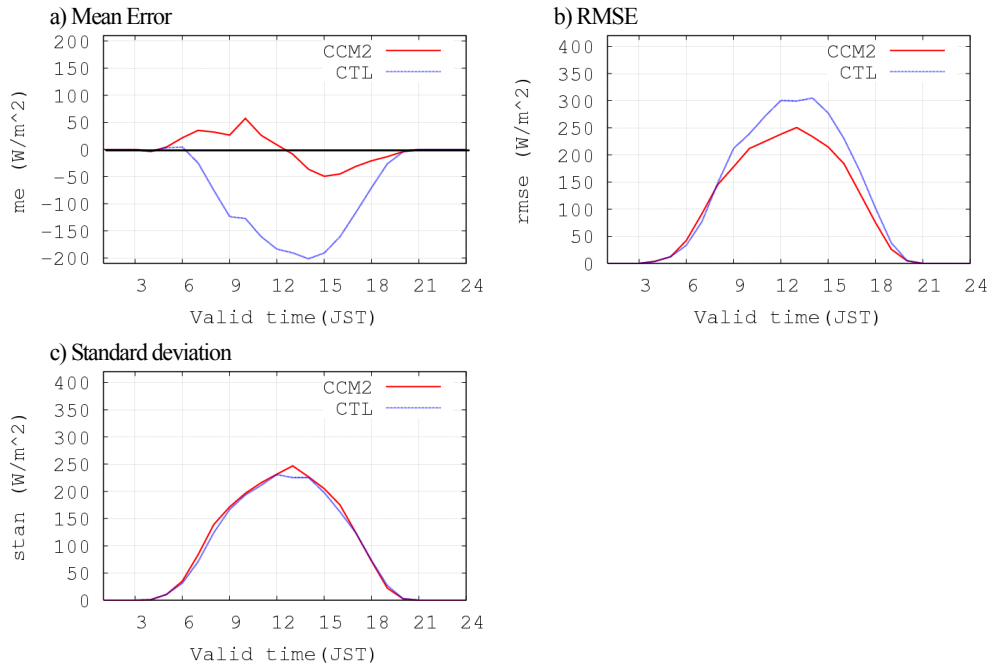

Fig. 4 a) Mean Error, b) RMSE, C) standard deviation, as a function of valid time, of the downward shortwave radiation flux (Wm^{-2}) at surface through experimental period by CCM2 (red) and CTL (blue) verified against data from surface observation of JMA.

6. REFERENCES

Briegleb, B. P., 1992: Delta-Eddington approximation for solar radiation in the NCAR community climate model. *J. Geophys. Res.,* 97, 7603-7612.

Ebert, E. E., and J. A. Curry, 1992: A parameterization of ice cloud optical properties for climate models, *J. Geophys. Res.,* 97, 3831-3836.

Goody, R. M., 1952: A statistical model for water vapor absorption. *Quart. J. Roy. Meteor. Soc.,* 78, 165-169.

Hack, J. J., 1998: Sensitivity of the simulated climate to a diagnostic formation for cloud liquid water. *J. Climate,* 11, 1497-1515.

Kiehl, J. T. and C. S. Zender, 1995: A Prognostic Ice Water Scheme for Anvil Clouds. World Climate Programme Research, WCRP-90, WMO/TD-No. 713, 167-188.

Kitagawa, H., 2000: Radiation scheme. *Report of Numerical Prediction Division,* 46, 16-31 (in Japanese, Suuchiyohouka Bessatsu Houkoku).

Ohno, H. and M. Isa, 1984: A statistical relation between GMS-viewed cloud amount and relative humidity. *Tenki,* 31, No.8, 493-495 (in Japanese).

Saito, K., T. Fujita, Y Yamada, J. Ishida, Y. Kumagai, K. Aranami, S. Ohmori, R. Nagasawa, S. Kumagai, C. Muroi, T. Kato, H. Eito and Y. Yamazaki, 2006: The operational JMA Nonhydrostatic Mesoscale Model. *Mon. Wea. Rev.,* **134,** 1266-1298.

Slingo, A., 1989: A GCM parameterization for the shortwave radiative properties of water clouds. *J. Atmos. Sci.,* 46, 1419-1427.

Slingo, J. M., 1987: The development and verification of a cloud prediction scheme for the ECMWF model. *Quart. J. Roy. Meteor. Soc,* 113, 899-927.